JOURNAL OF MATERIALS SCIENCE 25 (1990) 1509–1512

The microstructure of rapidly solidified Ti–32 wt % Fe melt-spun ribbon

I. LEVI, D. SHECHTMAN
Materials Engineering, Technion, Haifa, Israel

A Ti–32 wt % Fe alloy was rapidly solidified by the melt-spinning technique. Three microstructures are found in the melt-spun ribbon of the alloy: the first contains small FeTi particles in a β matrix, the second is a cellular microstructure composed of β and FeTi and the third is a eutectic of these phases. The correlation between various solidification and cooling rates across the ribbon width to the three microstructures is explained.

1. Introduction

Rapid solidification enables fine microstructures, extension solid solutions, metastable phases and amorphous phases to be obtained [1]. In this study we have examined the titanium-rich eutectic in the Ti–Fe binary system (Fig. 1) [2] with the purpose of characterizing the microstructure of the rapidly solidified Ti–32 wt % Fe melt-spun ribbon and correlating it with the solidification conditions.

Krishnamurthy *et al.* [3] and Baeslack *et al.* [4] examined the microstructures of some other Ti–Fe melt-spun ribbons, and it was found that β can form as a single phase in alloys with up to 22 wt % Fe. Ray *et al.* [5] found single-phase Ti–Fe alloys with up to 50 at % Fe made by splat cooling. Their conclusions were based on X-ray diffraction. Because of the absence of superlattice lines in the X-ray diffraction of the TiFe (CsCl structure type [6, 7]) and the similarity between the lattice parameters of the β solid solution and the TiFe (summarized in [2]), transmission electron microscopy (TEM) is a better technique to determine whether these alloys are really single phase. In the melt-spinning process the solidification rate changes across the ribbon as a function of the distance from the wheel. The highest solidification rate is obtained on the wheel side of the ribbon, where the temperature of the solid-liquid interface is the lowest. On the free side of the ribbon, the interface temperature is higher, due to the emission of heat of recalescence, and the solidification rate is therefore slower [8]. This change in the solidification rate across the ribbon results in different microstructures at the same composition, as will be shown in this work.

The phases found in this study are β-Ti, FeTi and ω-Ti. The β phase is stable at high temperatures (see Fig. 1) and can be also obtained as a metastable phase at room temperature by quenching Ti–Fe alloys with more than 4 at % Fe according to Moiseev [9] or 9.3 at % Fe according to Da Silva *et al.* [10]. It has a bcc structure with lattice parameter between 0.3196 nm in Ti–10 at % Fe and 0.3056 nm in Ti–35 at % Fe [5].

The ω phase is metastable with an hexagonal lattice. It can be obtained as a result of several processes. Among the various types are athermal ω forms obtained by quenching Ti–4 to 6 wt % Fe [11, 12] and isothermal ω which forms by ageing the β at high temperatures ($\approx 450°$ C) [11–13]. In both cases the composition of the ω is about 4 to 6 wt % Fe [13–15]. If the solute concentration is higher than the critical one, or the temperature is too high (above the transition temperature), then diffuse ω is obtained by quenching. This phase is characterized by diffuse streaking in the electron diffraction pattern [11, 12], and short-range atomic displacements of the β rather than discrete ω particles, are observed [12].

TiFe is a stable phase with compositions in the range 47.5 to 50.3 wt % Fe at the eutectic temperature [2]. It can be obtained as a metastable, non-stoichiometric phase by quenching [5]. TiFe has a CsCl structure with a lattice parameter of 0.2976 nm in the stoichiometric composition [6, 7].

2. Experimental procedure

The alloy was made by melting 99.97% pure components in an arc furnace. Rapidly solidified ribbon was made by melt-spinning in a helium atmosphere on an iron wheel spinning at a linear velocity of 40 m sec^{-1}. The ribbon obtained was 1 to 3 mm wide and 20 to 30 μm thick. The microstructure was examined by optical and transmission electron microscopy.

3. Results

The microstructure of the rapidly solidified Ti–32 wt % Fe ribbon is shown in Fig. 2. Most of the volume of the ribbon is composed of columnar grains, parallel to the heat flow direction, which grow from the wheel side. At the edge of the cross-section, on the side far from the wheel, the grains are equiaxed. The length of the columnar grains is about 25 μm, and their width 2.0 $\pm$ 0.5 μm. The average diameter of the equiaxed grains is 1.0 $\pm$ 0.3 μm.

Three different microstructures are found in the TEM study. The first is a cellular structure of the β phase with FeTi in the cell boundaries. FeTi also

0022–2461/90 $03.00 + .12

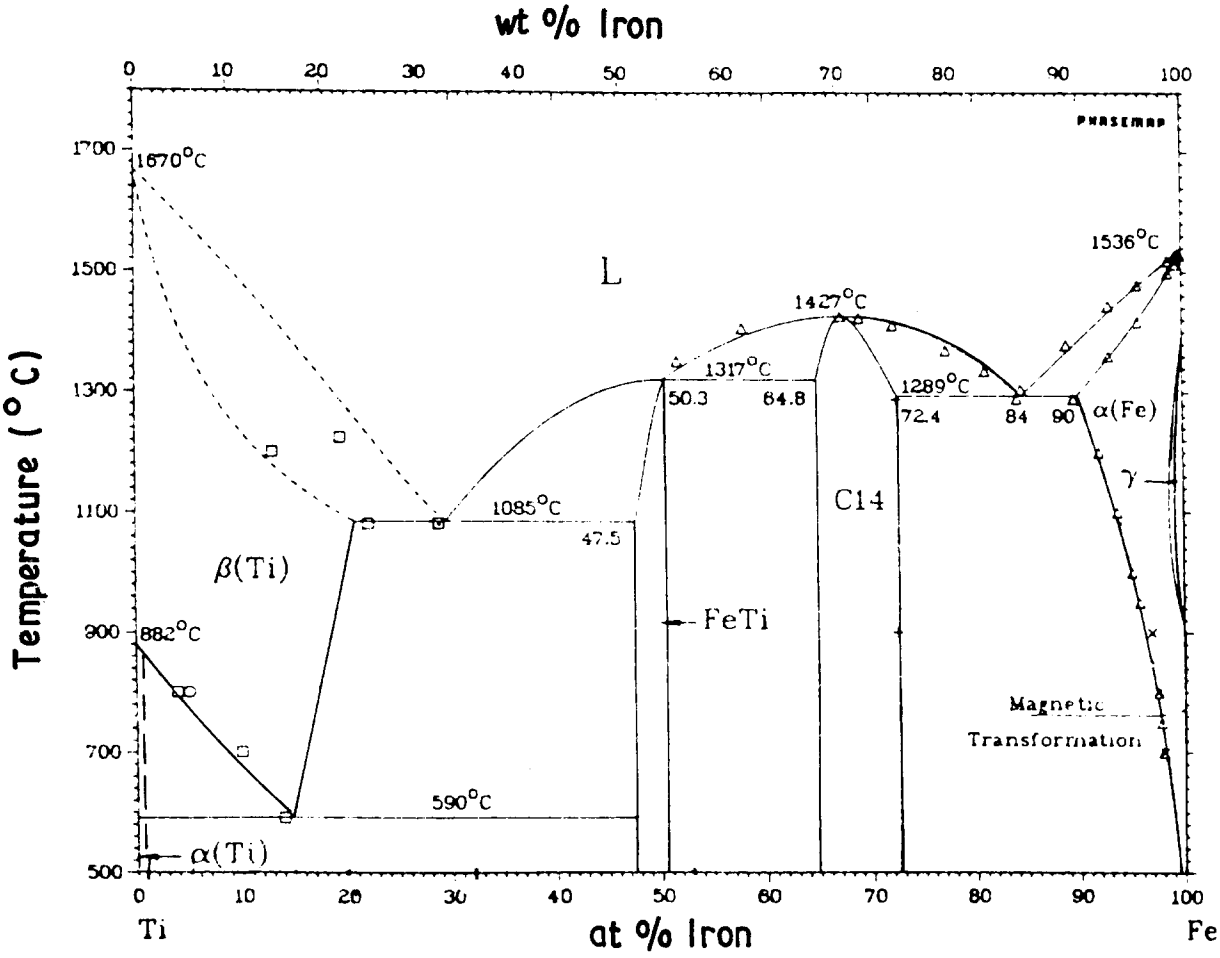

Figure 1 The Ti–Fe phase diagram [2].

appears as particles within these cells. The microstructure is shown in Fig. 3, and its electron diffraction pattern in Fig. 4. The electron diffraction pattern indicates the coherency between the FeTi particles and the β matrix. The orientation relationship between the β and the FeTi is determined to be:

$$[1\,0\,0]_{FeTi} \| [1\,0\,0]_{\beta}$$

$$(1\,1\,0)_{FeTi} \| (1\,1\,0)_{\beta}$$

The size of the cells is 200 to 400 nm and the size of the particles is 63.5 ± 9.0 nm long and 30.0 ± 5.0 nm wide.

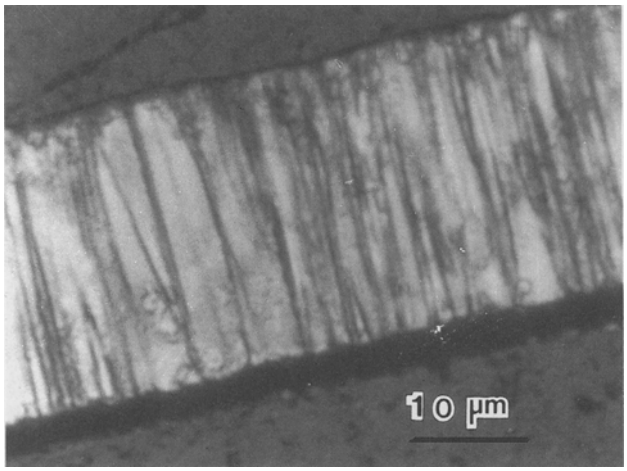

Figure 2 Optical micrograph of a cross-section of the Ti–32 wt % Fe ribbon.

The second microstructure is a coarse eutectic of β and TiFe (Fig. 5). An electron diffraction pattern from this region shows these two phases and also the diffuse streaking of the ω phase (Fig. 6). The orientation relationship between β and FeTi in this area is identical to that found in the cellular structure.

The third microstructure is composed of small FeTi particles in a β matrix (Fig. 7). The particle size is smaller than that observed in the cellular structure: the length of the particles is 35.0 ± 3.0 nm and their width is 16.0 ± 2.5 nm.

4. Discussion

The three microstructures obtained at the same melt-spun ribbon result from different solidification rates. The microstructure of the β matrix with small particles of FeTi is obtained upon solidification at the highest rate. In this case, β is solidified from the melt as a single phase in a segregation-free solidification mode. The FeTi particles precipitate by a solid-state transformation during the cooling process that follows.

As stated above, Ray *et al.* [5] also found β single phase in an alloy of this composition made by splat cooling. They did not find the TiFe solid-state transformation particles as we did, but this may be due to the limitations of the X-ray diffraction technique, as no transmission microscopy was used in this study.

The two other microstructures are obtained at slower solidification rates as can be deduced from the segregation of second phases. The medium solidification

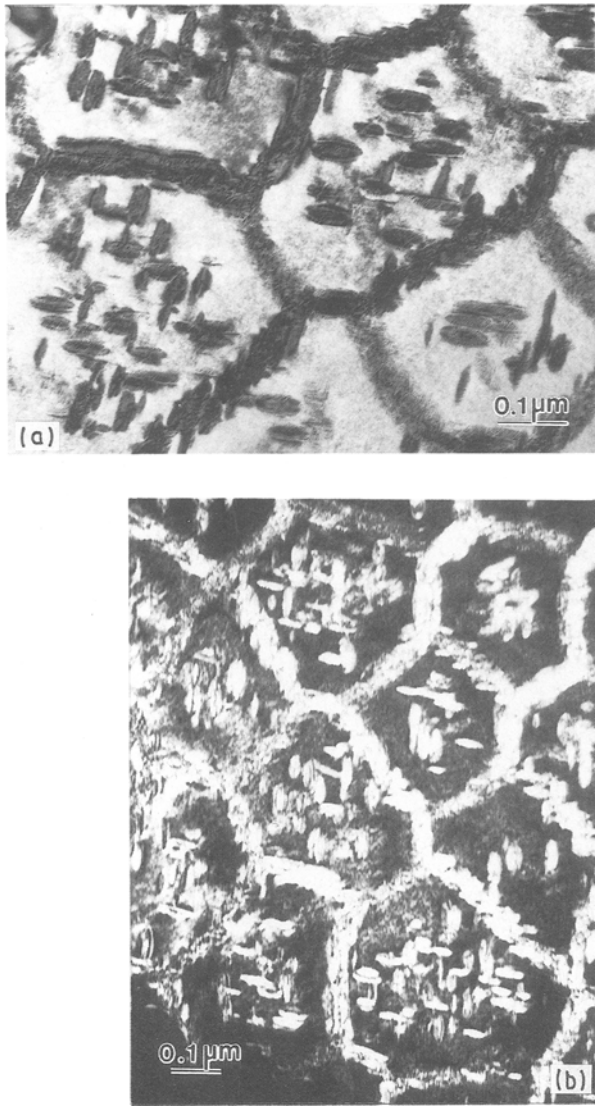

Figure 3 (a) Bright-field image of the cellular microstructure. (b) Dark-field image of the cellular microstructure, showing FeTi particles within the cells and in the cells boundaries (light) and the β matrix (dark).

rate causes the formation of the cellular microstructure. In this case the cells form during the solidification process, while the FeTi particles within the cells and at the cell boundaries are a result of a solid state transformation. The FeTi particles within the cellular microstructure are larger than the particles which

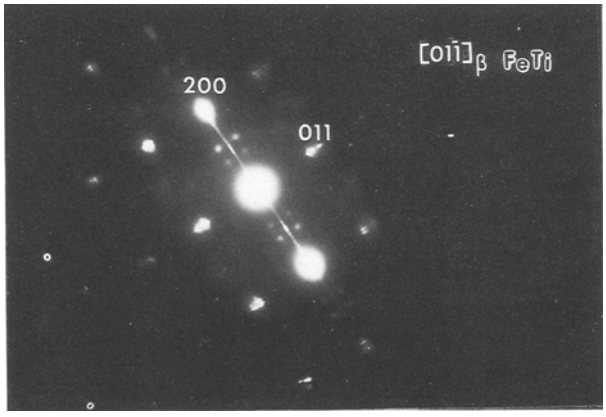

Figure 4 Selected-area pattern of the cellular area, showing β and TiFe phases.

Figure 5 Bright-field image of the eutectic area.

form in the single β phase which also indicates the difference in the solidification and cooling patterns between the two microstructures.

The coarse eutectic is obtained apparently as a result of the slowest solidification rate. In this equilibrium microstructure, the diffused streaks of the ω are seen in addition to the diffraction spots from the β and TiFe phases. It is known that the ω phase contains about 4 to 6 wt % Fe [11–13], therefore the range of compositions at the eutectic is wider than at the other microstructures, which can be expected from the slowest solidification rate of this microstructure.

5. Conclusions

Three different microstructures form in the Ti–32 wt % Fe melt-spun ribbon as a result of various solidification rates. The highest solidification rate results in the formation of a single β phase, while the slower rates result in segregation of second phases.

During the cooling process that follows the solidification, solid state transformation occurs in the two

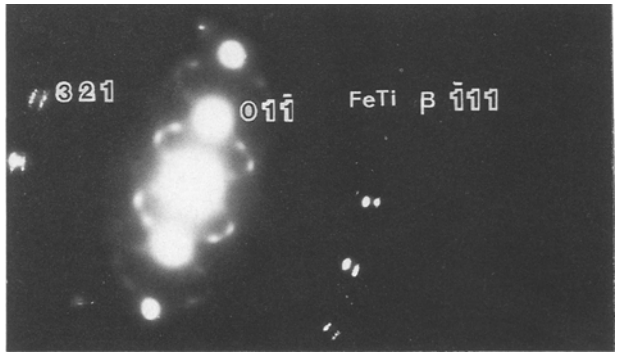

Figure 6 SAD pattern of the eutectic area, showing β and TiFe phases and diffuse streaking of ω phase.

Figure 7 Bright-field image showing FeTi particles in the β matrix.

microstructures which form by the two highest solidification rates. This solid state transformation results in the precipitation of TiFe particles from the β matrix.

Acknowledgements

We thank F. S. Biancaniello of NBS for the preparation of the alloy and ribbon. We also acknowledge the use of equipment in the SACHS centre at the Technion and the support of the National Council for Research and Development.

References

1. M. COHEN, B. H. KEAR and R. MEHRABIAN, in "Rapid Solidification. Principles and Technologies II", edited by R. Mehrabian, B. H. Kear, M. Cohen (Claitors, Baton Rouge, 1980) p. 1.
2. J. L. MURRAY, *Bull. Alloy. Ph. Diagrams* **2** (1981) 320.
3. S. KRISHNAMURTHY, R. G. VOGT, D. EYLON and F. H. FROES, in "Materials Research Society Proceedings, Vol. 28 edited by B. H. Kear and B. C. Giessen (Elsevier, New York, 1984) p. 361.
4. W. A. BAESLACK III, L. WEETER, S. KRISHNAMURTHY, P. SMITH and F. H. FROES, *ibid.*, p. 375.
5. R. RAY, B. C. GIESSEN and N. J. GRANT, *Met. Trans.* **3** (1972) 627.
6. T. V. PHILIP and P. A. BECK, *Trans. AIME J. Met.* **9** (1957) 1269.
7. P. DUWEZ and J. L. TAYLOR, *Trans. AIME J. Met.* **188** (1950) 1173.
8. R. C. RUHL, *Mater. Sci. Engng.* **1** (1967) 313.
9. V. N. MOISEEV, *Met. Sci. Heat Treat.* **5** (1969) 335 (translation).
10. E. G. DA SILVA, R. S. PRESTON and U. GONSER, *J. Appl. Phys.* **57** (1985) 1063.
11. T. W. DUERG, G. T. TERLINDE and J. C. WILLIAMS, in "Ti–80 Science and Technology", edited by H. Kimura and O. Izumi (TMS-AIME Warrendale, Pennsylvania, 1981) p. 1299.
12. D. DE FONTAINE, N. E. PATON and J. C. WILLIAMS, *Acta Metall.* **19** (1971) 1153.
13. B. S. HICKMAN, *Trans. Met. Soc. AIME* **245** (1969) 1329.
14. L. N. GUSEVA and L. K. DOLINSKAYA, *Russ. Met.* **6** (1974) 155 (translation).
15. L. P. ODINOKOVA and B. A. BRUSILOVSIY, *Phys. Met. Metallogr.* **31** (1971) 41 (translation).

Received 15 November 1988
and accepted 26 April 1989